Journal of Sound and Vibration (2002) **256**(5), 861–872
doi:10.1006/jsvi.5024, available online at http://www.idealibrary.com on IDEAL®

PIEZO–BEAM SYSTEMS SUBJECTED TO WEAK ELECTRIC FIELD: EXPERIMENTS AND MODELLING OF NON-LINEARITIES

U. VON WAGNER AND P. HAGEDORN

Department of Applied Mechanics, Darmstadt University of Technology, Hochschulstrasse 1, 64289 *Darmstadt, Germany. E-mail: wagner@mechanik.tu-darmstadt.de*

(*Received* 17 *May* 2001, *and in final form* 3 *October* 2001)

Typical non-linear effects, e.g., dependence of the resonance frequency on the amplitude, superharmonics in spectra and a non-linear relationship between excitation voltage and vibration amplitude are observed in experiments with piezoceramics and in piezo–beam systems excited at resonance by *weak* electric fields. These non-linear effects can be observed for both the piezoelectric 31 and the 33-effect. In contrast to the well-known non-linear effects for piezo-ceramics in the presence of *strong* electric fields, our findings have not been described yet in detail in the literature. In this paper, a first description of these phenomena is given by formulating non-linear constitutive relations, in particular by introducing a non-constant Young's modulus E_c and piezo electric factor d_{31} in the case of a piezo–beam system. The equations of motion for the system under consideration are derived via the Ritz method using Hamilton's principle. The "non-linear" parameters are determined and the numerical results are compared to those obtained experimentally. A finite element model is used for verification of the results obtained by the Ritz method. The effects described herein may have a significant influence whenever structures are excited close to resonance frequencies via piezoelectric elements.

1. INTRODUCTION

Figure 1 shows the system under consideration consisting of a cantilever beam with length l, width b, and height h_b. The lateral deformation of this beam is described by $w(x, t)$. Two piezoceramics are bonded to the beam at mid-length (PIC 151 manufactured by PI-Ceramic at Lederhose, Germany, z direction is the polarization direction). The dimensions of the piezoceramics are given in Figure 1, the width is equal to that of the beam. The parameter values used in the experiment are given in Section 5. The piezo–beam system is excited to bending vibrations close to the first two resonance frequencies by applying a corresponding alternate voltage with amplitude U_0.

The observed behavior was typical of non-linear systems and included e.g., amplitude-dependence of the resonance frequency, superharmonics in the response spectra and a non-linear relationship between excitation voltage and vibration amplitude. A typical non-linear response observed in the experimental set-up is shown in Figure 2. This figure clearly shows a non-linear relationship between excitation voltage and amplitude response at the first natural frequency. The natural frequency is determined at low voltages where the behavior is approximately linear. Compared with an imaginary linear behavior in this figure, these non-linear effects may result in differences in amplitude values of up to 200%. This will be the case, if the system is excited at a natural frequency at low voltages, and the

0022-460X/02/$35.00

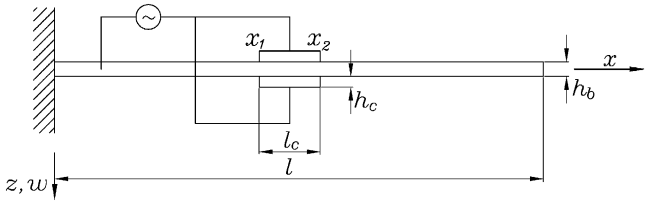

Figure 1. Piezo–beam system.

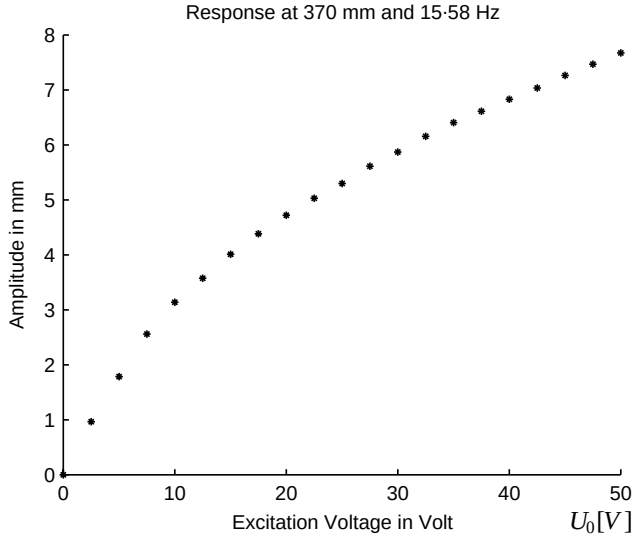

Figure 2. Back-bone curve (amplitude response, excitation frequency $f = 15{\cdot}58$ Hz (first natural frequency): ●, experiment.

applied voltage is increased. They should for this reason not be neglected in the design of smart structures or in the optimization of energy transfer when using such elements.

The current study presents observations of non-linear effects of this piezo–beam system subjected to weak electric fields. In contrast, the non-linear behavior of piezoceramics in the presence of strong electric fields is a well-known phenomenon. Dielectric hysteresis and butterfly hysteresis are typical examples [1–3]. Hysteresis phenomena are also observed using piezoelectric stack actuators [4]. The non-linear behavior of piezoceramics subjected to weak electric field, as far as we know, has not been described in detail in the literature. The non-linear behavior of piezo–beam systems subjected to weak electric field e.g., was mentioned by Crawley and de Luis [5], who attributed it to non-linear damping.

2. POSSIBLE REASONS FOR NON-LINEAR BEHAVIOR

Nguyen [6] investigated several possibilities for explaining the non-linear behavior found in piezo–beam systems, focusing on four main aspects: damping, influence of the adhesive layer, non-linear beam theories and non-linear elastic and coupling behavior of the piezoceramic.

Experiments with vibrations of free piezoceramics showed that the damping is small within the piezoceramic. On the other hand, experiments with free and forced vibrations of

the beam showed that a *linear* damping law provides a sufficiently accurate description of the damping behavior.

The influence of the adhesive layer was also investigated by Nguyen [6] experimentally, exciting the piezo–beam system by a harmonic force applied at the free end of the cantilever beam. The resulting strains in the beam and piezoceramic were measured and a linear relationship was observed.

In order to examine a possible non-linear behavior of the beam itself, different non-linear beam theories were considered. The case of a cantilever beam including the effect of longitudinal inertia was first investigated. This had been shown to result in a softening effect by Atluri [7]. These results show the same qualitative softening behavior as found in our experiment; however, in the case of the experiment, the effect was much stronger than could possibly explained by this theory. Softening was also observed in tests on a piezo–beam system with both end clamped, despite the fact that *stiffening* due to geometrical non-linear behavior is expected in this case [8, 9]!

Obviously, the measured non-linear behavior is not described correctly by the effects discussed so far. Hence, we concentrated on a non-linear elastic and coupling behavior of the piezoceramic resulting in the development of the non-linear piezo–beam model given in the next section. Experiments with forced vibrations of free piezoceramics electrically excited close to their natural frequencies [6] showed a non-linear, unsymmetric strain-dependent behavior of the Young's modulus E_c and the piezoelectric factor d_{31}. These experiments are taken into account in developing the extension of the electric enthalpy density for the non-linear effects.

3. NON-LINEAR MODELLING

In order to derive the equations of motion, Hamilton's principle can be used. For a piezoelectric continuum, it can be formulated as [10]

$$\delta \int_{t_0}^{t_1} L \, \mathrm{d}t + \int_{t_0}^{t_1} \delta W \, \mathrm{d}t = 0 \tag{1}$$

with the Langrangian

$$L = \int_V (T - H) \, \mathrm{d}V,$$

where T and H, respectively, denote the kinetic energy density and the electric enthalpy density. In the linear case, the enthalpy is given by [10]

$$H = \tfrac{1}{2} E_c S_{xx}^2 - E_c d_{31} S_{xx} E_z - \tfrac{1}{2}(\varepsilon_{33}^{\mathrm{T}} - d_{31}^2 E_c) E_z^2, \tag{2}$$

where S_{xx} is the strain with respect to the x direction, E_c Young's modulus of the piezoceramic and E_z the electric field in the z direction. The parameter d_{31} corresponds to the piezoelectric 31-effect and $\varepsilon_{33}^{\mathrm{T}}$ is the dielectric constant measured at constant stress. Using

$$T_{xx} = \frac{\partial H}{\partial S_{xx}} \quad \text{and} \quad D_z = -\frac{\partial H}{\partial E_z}, \tag{3}$$

where D_z is the electric displacement with respect to the z direction and T_{xx} the stress with respect to the x direction, the well-known linear constitutive equations

$$T_{xx} = E_c S_{xx} - d_{31} E_c E_z, \tag{4}$$

$$D_z = d_{31} E_c S_{xx} + (\varepsilon_{33}^{\mathrm{T}} - d_{31}^2 E_c) E_z \tag{5}$$

are derived.

Based on experimental results [6], the non-linear dependence of E_c and d_{31} on S_{xx} is approximated by

$$E_c = E_c^{(0)} + E_c^{(1)} S_{xx} + E_c^{(2)} S_{xx}^2, \tag{6}$$

$$d_{31} = d_{31}^{(0)} + d_{31}^{(1)} S_{xx} + d_{31}^{(2)} S_{xx}^2. \tag{7}$$

Assuming a linear relation between D_z and E_z and retaining terms only up to the third order, the electric enthalpy density is derived as

$$\begin{aligned} H = {} & \tfrac{1}{2} E_c^{(0)} S_{xx}^2 + \tfrac{1}{3} E_c^{(1)} S_{xx}^3 + \tfrac{1}{4} E_c^{(2)} S_{xx}^4 \\ & - \gamma_0 S_{xx} E_z - \tfrac{1}{2} \gamma_1 S_{xx}^2 E_z - \tfrac{1}{3} \gamma_2 S_{xx}^3 E_z - \tfrac{1}{2} v_0 E_z^2 \end{aligned} \tag{8}$$

with

$$\begin{aligned} v_0 &= \varepsilon_{33}^{\mathrm{T}} - (d_{31}^{(0)})^2 E_c^{(0)}, \qquad \gamma_0 = E_c^{(0)} d_{31}^{(0)}, \\ \gamma_1 &= E_c^{(0)} d_{31}^{(1)} + E_c^{(1)} d_{31}^{(0)}, \quad \gamma_2 = E_c^{(0)} d_{31}^{(2)} + E_c^{(2)} d_{31}^{(0)} + E_c^{(1)} d_{31}^{(1)}, \end{aligned} \tag{9}$$

which satisfies the necessary and sufficient condition for the existence of the enthalpy function:

$$\frac{\partial^2 H}{\partial S_{xx} \partial E_z} = \frac{\partial T_{xx}}{\partial E_z} = -\frac{\partial D_z}{\partial S_{xx}} = \frac{\partial^2 H}{\partial E_z \partial S_{xx}}. \tag{10}$$

Using equation (3), the non-linear constitutive equations (4) and (5) can be derived from (8)

$$\begin{aligned} T_{xx} = {} & E_c^{(0)} S_{xx} + E_c^{(1)} S_{xx}^2 + E_c^{(2)} S_{xx}^3 \\ & - \gamma_0 E_z - \gamma_1 S_{xx} E_z - \gamma_2 S_{xx}^2 E_z, \end{aligned} \tag{11}$$

$$D_z = \gamma_0 S_{xx} + \tfrac{1}{2} \gamma_1 S_{xx}^2 + \tfrac{1}{3} \gamma_2 S_{xx}^2 + v_0 E_z. \tag{12}$$

The virtual work δW in the undamped case vanishes:

$$\delta W = 0. \tag{13}$$

4. EQUATIONS OF MOTION

In order to derive the equations of motion using Hamilton's principle, H has to be integrated over the volume of the beam and the piezoceramic to calculate L,

$$\begin{aligned} \int_V H \, \mathrm{d}V &= \int_{V_b} H \, \mathrm{d}V + \int_{V_c} H \, \mathrm{d}V \\ &= \int_{V_b} \frac{1}{2} E_b S_{xx}^2 \, \mathrm{d}V + \int_{V_c} \left(\frac{1}{2} E_c^{(0)} S_{xx}^2 + \frac{1}{3} E_c^{(1)} S_{xx}^2 + \frac{1}{4} E_c^{(2)} S_{xx}^4 \right. \\ &\quad \left. - \gamma_0 s_{xx} E_z - \frac{1}{2} \gamma_1 S_{xx}^2 E_z - \frac{1}{3} \gamma_2 S_{xx}^3 E_z - \frac{1}{2} v_0 E_z^2 \right) \mathrm{d}V, \end{aligned} \tag{14}$$

where E_b is Young's modulus of the beam. The terms containing $E_c^{(1)}$ and γ_1 vanish due to the symmetry of the system (see Section 7) and the fact, that the electric field E_z has

opposite signs within the two piezoceramics. Using the kinematic relation

$$S_{xx}(x,z,t) = -\frac{\partial^2 w(x,t)}{\partial x^2} z, \quad \forall x \in [0,l], \quad \forall z \in \left[-\frac{h_b}{2} - h_c, \frac{h_b}{2} + h_c\right], \tag{15}$$

due to Euler–Bernoulli beam theory, the electric enthalpy is given as

$$\begin{aligned}\int_V H \,\mathrm{d}V = &\frac{1}{2} E_b I_b \int_0^t (w'')^2 \,\mathrm{d}x + 2a_1 \int_{x_1}^{x_2} (w'')^2 \,\mathrm{d}x + 2a_3 \int_{x_1}^{x_2} (w'')^4 \,\mathrm{d}x \\ &+ 2b_1 \left(\int_{x_1}^{x_2} w'' \,\mathrm{d}x\right) E_z + 2b_3 \left[\int_{x_1}^{x_2} (w'')^3 \,\mathrm{d}x\right] E_z - 2b_0 E_z^2\end{aligned} \tag{16}$$

with

$$\begin{aligned}a_1 &= \frac{1}{6} E_c^{(0)} b \left[\left(\frac{h}{2} + h_c\right)^3 - \left(\frac{h}{2}\right)^3\right], \quad a_3 = \frac{1}{20} E_c^{(2)} b \left[\left(\frac{h}{2} + h_c\right)^5 - \left(\frac{h}{2}\right)^5\right], \\ b_0 &= \frac{1}{2} v_0 b h_c l_c, \quad b_1 = \frac{1}{2} \gamma_0 b \left[\left(\frac{h}{2} + h_c\right)^2 - \left(\frac{h}{2}\right)^2\right], \\ b_3 &= \frac{1}{12} \gamma_2 b \left[\left(\frac{h}{2} + h_c\right)^4 - \left(\frac{h}{2}\right)^4\right].\end{aligned} \tag{17}$$

The kinetic energy of the piezo–beam system is obtained by

$$\int_V T \,\mathrm{d}V = \frac{1}{2} \int_V \rho \dot{w}^2 \,\mathrm{d}V = \frac{1}{2} \rho_b A_b \int_0^l \dot{w}^2(x,t) \,\mathrm{d}x + \rho_c A_c \int_{x_1}^{x_2} \dot{w}^2(x,t) \,\mathrm{d}x. \tag{18}$$

Introducing equations (16), (18) and (13) into Hamilton's principle results in

$$\begin{aligned}\delta \int_{t_0}^{t_1} L \,\mathrm{d}t = \delta \int_{t_0}^{t_1} \Bigg\{ &\left[\frac{1}{2} \rho_b A_b \int_0^l (\dot{w})^2 \,\mathrm{d}x + \rho_c A_c \int_{x_1}^{x_2} (\dot{w})^2 \,\mathrm{d}x\right] \\ &- \Bigg\{\frac{1}{2} E_b I_b \int_0^l (w'')^2 \,\mathrm{d}x + 2a_1 \int_{x_1}^{x_2} (w'')^2 \,\mathrm{d}x + 2a_3 \int_{x_1}^{x_2} (w'')^4 \,\mathrm{d}x \\ &+ 2b_1 \left(\int_{x_1}^{x_2} w'' \,\mathrm{d}x\right) E_z + 2b_3 \left[\int_{x_1}^{x_2} (w'')^3 \,\mathrm{d}x\right] E_z - 2b_0 E_z^2 \Bigg\} \Bigg\} \,\mathrm{d}t = 0.\end{aligned} \tag{19}$$

4.1. LINEAR CASE

The eigenfunctions of the linear problem are calculated in this section. They are used as shape functions for the non-linear case in the next section. The non-linear parameters a_3 and b_3 are assumed to be equal to zero in this case.

The electric field is considered to be homogeneous ($E_z \neq f(x)$) and to be due to an external excitation ($\delta E_z = 0$). The beam is divided into three segments with lateral deformations w_1, w_2, w_3 for the regions $0 < x \leqslant x_1, x_1 < x \leqslant x_2, x_2 < x \leqslant l$ respectively. The boundary value problem is given by three equations of motion

$$E_b I_b w_1'''' + \rho_b A_b \ddot{w}_1 = 0, \tag{20}$$

$$(E_b I_b + 2a_1) w_2'''' + (\rho_b A_b + 2\rho_c A_c) \ddot{w}_2 = 0, \tag{21}$$

$$E_b I_b w_3'''' + \rho_b A_b \ddot{w}_3 = 0 \tag{22}$$

and 12 boundary conditions

$$w_1(0,t)=0, \quad w_1'(0,\tau)=0,$$

$$w_1(x_1,t)=w_2(x_1,t), \quad w_1'(x_1,t)=w_2'(x_1,t),$$

$$(E_bI_b+2a_1)w_2''(x_1,t)-E_bI_bw_1''(x_1,t)+b_1E_z(t)=0,$$

$$E_bI_bw_1''(x_1,t)-(E_bI_b+2a_1)w_2''(x_1,t)=0,$$

$$w_2(x_2,t)=w_3(x_2,t), \quad w_2'(x_2,t)=w_3'(x_2,t)=w_3'(x_2,t),$$

$$-(E_bI_b+2a_1)w_2''(x_2,t)+E_bI_bw_3''(x_2,t)+b_1E_z(t)=0,$$

$$-E_bI_bw_3'''(x_2,t)+(E_bI_b+2a_1)w_2'''(x_2,t)=0,$$

$$w_3''(l,t)=0, \quad w_3'''(l,t)=0.$$

Considering the case of short-circuited electrodes of the piezoceramics ($E_2=0$), the eigenfunctions $W_k(x)$ of the piezo–beam can be obtained using the general solution

$$\begin{aligned} W_{ik}(x) &= A_{ik}\sin\lambda_{ik}x+B_{ik}\cos\lambda_{ik}x+C_{ik}\sinh\lambda_{ik}x+D_{ik}\cosh\lambda_{ik}x,\\ i &= 1,2,3, \quad k=1,2,\ldots,\infty \end{aligned} \tag{23}$$

with

$$\lambda_{1k}^4=\lambda_{3k}^4=\frac{\rho_bA_b}{E_bI_b}\omega_k^2, \quad \lambda_{2k}^4=\frac{(\rho_bA_b+2\rho_cA_c)}{(E_bI_b+2a_1)}\omega_k^2,$$

where ω_k is the kth circular eigenfrequency which can be determined in addition to the constants A, B, C, D by introducing equation (23) into the time-independent boundary conditions.

4.2. NON-LINEAR CASE

The constants a_3 and b_3 are no longer equal to zero in the non-linear case. According to the Rayleigh–Ritz method, the expansion

$$w(x,t)=\sum_k \Phi_k(x)p_k(t) \tag{24}$$

is introduced into equation (19). The shape functions $\Phi_k(x)$ are chosen as the eigenfunctions W_k calculated above. In contrast to references [6, 11], where the

eigenfunctions of the beam without piezoceramics are used, these shape functions provides much better convergence of the results, as described later in more detail.

Performing the variation, considering the orthogonality relations of the shape functions $\Phi_k(x)$ and assuming that $E_z = U(t)/h_c$ is homogeneous results in

$$\delta\int_{t0}^{t_1} L\,\mathrm{d}t = \sum_k \int_{t_0}^{t_1}\Big\{ -\rho_b A_b \ddot{p}_k \int_0^l \Phi_k^2\,\mathrm{d}x - 2\rho_c A_c \ddot{p}_k \int_{x_1}^{x_2} \Phi_k^2\,\mathrm{d}x$$
$$- E_b I_b p_k \int_0^l (\Phi_k'')^2\,\mathrm{d}x - 4a_1 p_k \int_{x_1}^{x_2} (\Phi_k'')^2\,\mathrm{d}x - 8a_3 \int_{x_1}^{x_2} \left(\sum_j p_j \Phi_j''\right)^3 \Phi_k''\,\mathrm{d}x$$
$$- 2b_1 E_z \int_{x_1}^{x_2} \Phi_k''\,\mathrm{d}x - 6b_3 E_z \int_{x_1}^{x_2} \left(\sum_j p_j \Phi_k''\right)^2 \Phi_k''\,\mathrm{d}x\Big\}\delta p_k\,\mathrm{d}t = 0. \tag{25}$$

In order to observe the non-linear effects, the system must be excited close to a natural frequency. Hence, it is sufficient to approximate the system using one shape function only, resembling the eigenform at the excitation frequency. Neglecting all coupling terms, the system of uncoupled differential equations is derived as

$$m_k \ddot{p}_k(t) + d_k \dot{p}_k(t) + c_k p_k(t) + \varepsilon_k^{(1)} p_k^3(t) + \varepsilon_k^{(2)} p_k^2(t) = f_k, \quad k = 1, 2, 3, \ldots \tag{26}$$

with

$$m_k = \rho_b A_b \int_0^l \Phi_k^2(x)\,\mathrm{d}x + 2\rho_c A_c \int_{x_1}^{x_2} \Phi_k^2(x)\,\mathrm{d}x,$$
$$c_k = E_b I_b \int_0^l (\Phi_k''(x))^2\,\mathrm{d}x + \frac{2}{3} E_c b \left[\left(\frac{h_b}{2} + h_c\right)^3 - \left(\frac{h_b}{2}\right)^3\right] \int_{x_1}^{x_2} (\Phi_k''(x))^2\,\mathrm{d}x,$$
$$f_k(t) = E_c^{(0)} b (h_b + h_c)[\Phi_k'(x_2) - \Phi_k'(x_1)] d_{31}^{(0)} U(t),$$
$$\varepsilon_k^{(1)} = \frac{4}{5} E_c^{(2)} b \left[\left(\frac{h_b}{2} + h_c\right)^5 - \left(\frac{h_b}{2}\right)^5\right] \int_{x_1}^{x_2} (\Phi_k'')^4\,\mathrm{d}x,$$
$$\varepsilon_k^{(2)} = \frac{1}{2}[d_{31}^{(1)} E_c^{(1)} + d_{31}^{(2)} E_c^{(0)} + d_{31}^{(0)} E_c^{(2)}] b \left[\left(\frac{h_b}{2} + h_c\right)^4 - \left(\frac{h_b}{2}\right)^4\right] \left[\int_{x_1}^{x_2} (\Phi_k'')^3\,\mathrm{d}x\right] \frac{U(t)}{h_c}, \tag{27}$$

the excitation voltage being

$$U(t) = U_0 \cos(\Omega t).$$

Herein, a Rayleigh-type linear modal damping $d_k \dot{p}_k(t)$ is added

$$d_k = \alpha m_k + \beta c_k. \tag{28}$$

The parameters α, β are derived experimentally.

4.3. SOLUTION BY THE HARMONIC BALANCE METHOD

For the determination of the non-linear coefficients, equation (26) is solved approximately and the vibration amplitude is found. This procedure must be rather fast so that it can be used in an optimization scheme for identification. A first approximate solution of the differential equation is obtained via the harmonic balance method. Equation (26) can be written as

$$m\ddot{p}(t) + d\dot{p}(t) + cp(t) + \varepsilon^{(1)} p^3(t) = F_0 \cos(\Omega t + \varphi) - \bar{\varepsilon}^{(2)} \cos(\Omega t + \varphi) p^2(t). \tag{29}$$

TABLE 1

	l (mm)	b (mm)	h (mm)	ρ (kg/m^3)	E (N/m^2)	d_{31}	Remark
Beam	400	25	3	7800	$2{\cdot}089 \times 10^{11}$	—	St 37
Piezo	70	25	1	7790	$0{\cdot}667 \times 10^{11}$	$-2{\cdot}1 \times 10^{-10}$	PIC 151

According to reference [12],

$$p(t) = A\cos(\Omega t) \tag{30}$$

is introduced. Neglecting higher harmonics, this results in a polynomial equation for the amplitude A

$$a_5(A^2)^5 + a_4(A^2)^4 + a_3(A^2)^3 + a^2(A^2)^2 + a_1A^2 + a_0 = 0 \tag{31}$$

with the coefficients

$$a_0 = -F_0^4,$$

$$a_1 = [(c - m\Omega^2)^2 + (d\Omega)^2]F_0^2 - \tfrac{1}{2}\bar{\varepsilon}^{(2)}F_0^3,$$

$$a_2 = [\tfrac{3}{2}(c - m\Omega^2)\varepsilon^{(1)} - \tfrac{11}{8}(\bar{\varepsilon}^{(2)})^2]F_0^2 - \tfrac{1}{2}[(c - m\Omega^2)^2 + 3(d\Omega)^2]\bar{\varepsilon}^{(2)}F_0,$$

$$a_3 = [\tfrac{1}{16}(c - m\Omega^2) + 9(d\Omega)^2](\bar{\varepsilon}^{(2)})^2 + \tfrac{9}{16}(\varepsilon^{(1)})^2F_0^2 - \tfrac{3}{4}(c - m\Omega^2)F_0\varepsilon^{(1)}\bar{\varepsilon}^{(2)} + \tfrac{3}{8}F_0(\bar{\varepsilon}^{(2)})^3,$$

$$a_4 = -\tfrac{9}{32}(\varepsilon^{(1)})^2\bar{\varepsilon}^{(2)}F_0 - \tfrac{9}{256}(\bar{\varepsilon}^{(2)})^4 + \tfrac{3}{32}(c - m\Omega^2)\varepsilon^{(1)}(\bar{\varepsilon}^{(2)})^2,$$

$$a_5 = \tfrac{9}{256}(\varepsilon^{(1)})^2(\bar{\varepsilon}^{(2)})^2, \tag{32}$$

which can be solved, e.g., using Matlab. For comparison, equation (26) was also solved by numerical integration, and good agreement was found.

5. DETERMINATION OF NON-LINEAR PARAMETERS

The linear parameters for the beam and the piezoceramic are given in Table 1.

The piezo–beam system is excited with the help of a function generator (Hewlett–Packard HP 33120 A). The signal from the function generator is amplified using a power amplifier (Brüel & Kjaer 2713, max voltage 100 V, max current 1 A, limit frequency 100 kHz). The vibrations of the beam are measured with the help of a laser vibrometer (Polytech). The excitation signal from the amplifier and from the vibrometer are fed to a digital scope (Yokogawa DL708E). The piezoceramics are bonded manually to the beam with the help of cyanacrylat adhesive (HBM Z70 rapid adhesive). The thickness of the bonding layer is smaller than 0·05 mm. At the clamped end, the beam is welded to a base which is fixed by screws at a foundation.

Figure 3 shows the measured response obtained by exciting the system with constant frequency $f = 15{\cdot}58$ Hz at different voltages. This first natural frequency is found at low voltages, where the behavior of the piezo–beam system is approximately linear. Subsequently, the applied voltage is increased at constant excitation frequency. This curve is used for the determination of the four non-linear parameters $d_{31}^{(1)}$, $d_{31}^{(2)}$, $E_c^{(1)}$ and $E_c^{(2)}$ by equation (31) via an optimization algorithm implemented in Matlab. The identified "non-linear" parameters are given in Table 2.

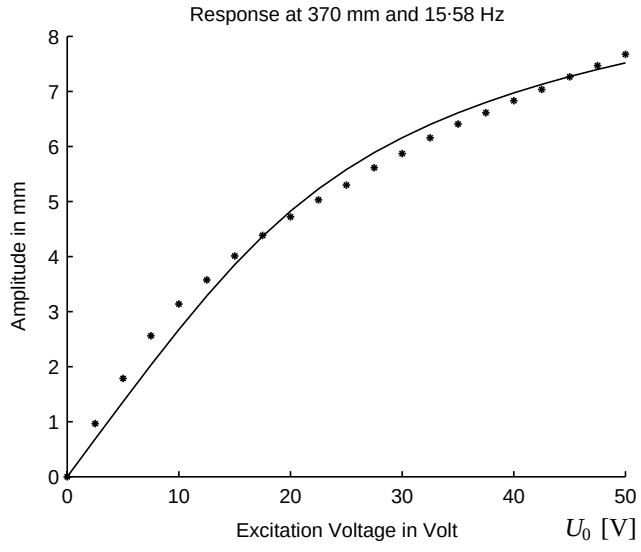

Figure 3. Amplitude response, excitation frequency $f = 15{\cdot}58\,\text{Hz}$ (first natural frequency), $x = 370\,\text{mm}$: —, theory; ●, experiment.

TABLE 2

$E_c^{(1)}$ (N/m^2)	$E_c^{(2)}$ (N/m^2)	$d_{31}^{(1)}$ (m/V)	$d_{31}^{(2)}$ (m/V)
$-3{\cdot}328 \times 10^{-12}$	$-1{\cdot}400 \times 10^{18}$	$-36{\cdot}9746$	$-0{\cdot}03596$

The damping coefficients α, β (equation (28)) are determined by the same procedure as used previously

$$\alpha = 0{\cdot}15/s, \quad \beta = 3{\cdot}165 \times 10^{-6}\,\text{s},$$

which are very close to "structural" damping as described in reference [13].

The closed line in Figure 3 represents the theoretical result obtained by the model described above, which is in good agreement with the measured data. The resonance amplitude at the second resonance frequency was also calculated using the parameters given in Table 2 in order to validate these results. For comparison, the maximum response amplitude was measured at second resonance frequency with different excitation voltages. Figure 4 shows measured and calculated results for this case, which clearly exhibit the softening character due to the non-linearities.

In order to lift the restriction imposed by using one shape function only, the amplitude was also calculated in several cases by numerical integration with up to four shape functions considering full non-linear coupling corresponding to equation (25). These results showed an excellent agreement with the result obtained with just one shape function resembling the eigenfunction close to the excitation frequency.

The results differ from those obtained by using the shape functions of the beam *without piezoceramics* [6, 11], where an increase in the number of shape functions used leads to a better approximation. The "reward" for the effort of deriving the eigenfunctions of the beam *including the piezoceramics* is therefore obvious!

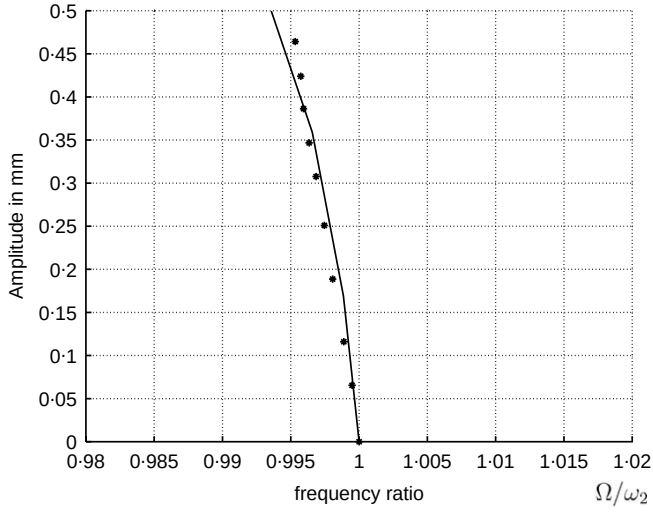

Figure 4. Back-bone curve (amplitude at $x = 370\,\text{mm}$ and resonance frequency near second natural frequency): —, theory; ●, experiment.

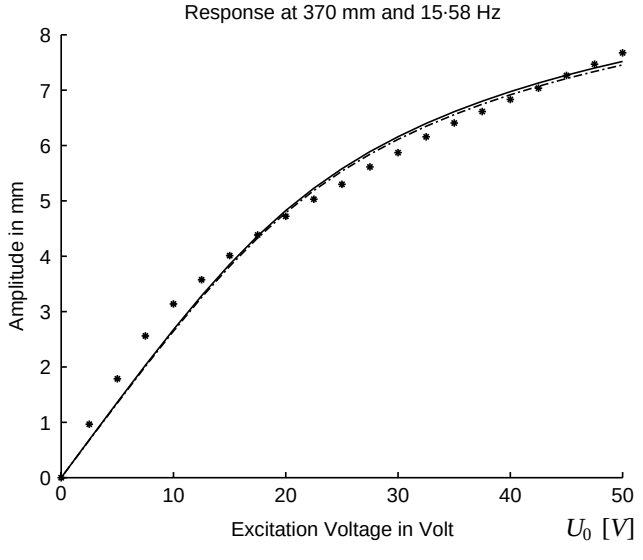

Figure 5. Amplitude response, excitation frequency $f = 15{\cdot}58\,\text{Hz}$ (first natural frequency, $x = 370\,\text{mm}$: —, theory; — —, FEM; ●, experiment.

6. FINITE ELEMENT MODEL

The theoretical results were also verified by using a finite element model developed by Parashar [14]. The derivation of the equations of motion follows the same steps up to equation (19), where instead of using expansion (24), the finite element method is used for discretization by simple one-dimensional beam elements. Figure 5 shows a comparison of results, corresponding to those of Figure 3, using three elements for the part with piezoceramics and 10 elements for the remaining part. The results of both theoretical methods show good agreement.

7. INFLUENCE OF ASYMMETRIES

Experiments of forced vibrations of free piezoceramics often show asymmetric behavior [6], e.g., peaks at even superharmonics in FFT-spectra. Due to the symmetric structure of the system under consideration (one piezoceramic bonded at each side of the beam respectively), the influence of the asymmetry of the piezoceramics vanish, as described above. This results in the fact that even superharmonics of the excitation frequency are not expected in light of equation (26). Consequently, this set-up seems to be ill-suited for the determination of the "asymmetric" parameters $d_{31}^{(1)}$, $E_c^{(1)}$, although they influence the cubic non-linearities of equation (26).

Nevertheless, even superharmonics are observed in the described experiments of the piezo–beam system. The authors attribute this effect to imperfections of the bonding and of the piezoceramics. Experiments with piezoceramics which were intentionally relatively shifted in the axial direction of the beam exhibited much higher peaks at even superharmonics in FFT-spectra! These results may be attributed to electrostrictive behavior, which is a well-known feature of piezoceramics. Electrostriction was not considered in the enthalpy density (8).

However, the observed non-linear behavior at resonance is clearly a result of cubic-like non-linearities as quadratic-like non-linearities have a minor influence.

8. CONCLUSIONS AND OUTLOOK

Typical non-linear effects were observed in experiments carried out with piezo–beam systems subjected to weak electric fields. In order to model the system appropriately, a non-linear *ansatz* was used for Young's modulus E_c and the piezoelectric factor d_{31}. The equations of motion for the system under consideration were derived by the Ritz method using Hamilton's principle. The non-linear parameters were determined and the results were validated through comparison with experiments.

The described effects may have significant influence on quantitative results and should not be neglected when such structures are excited close to resonance frequencies! Compared with references [6,11], the procedure could be improved by using improved shape functions leading to a significantly faster convergence of the results. The appearance of even superharmonics could be explained. One part of the authors' ongoing work is to decide whether such effects occur also with other types of piezoceramics and not only at the d_{31}-effect but also at the d_{33}-effect, for example. For this purpose, experiments with piezoceramics PIC181 manufactured by PI-Ceramic are being performed. In these experiments, slender (pure) piezoceramics with 20 mm length and a variety of cross-sections are excited to longitudinal vibrations. Figure 6 shows the result of an excitation with alternate voltage and an amplitude of 30 V. It clearly exhibits a non-linearity of the Duffing-type including a significant jump phenomenon!

It should be pointed out, that the described effect is, in fact, a non-linearity at weak electric fields. The maximum applied electric field amplitude in the experiments was $E_{max} = 5 \times 10^{-5}$ kV/m. For the well-known butterfly hysteresis, 2 kV/m are typical amplitudes! The same is correct for the strains. In reference [15], a butterfly hysteresis curve can be found for the material PIC 151, which were used in the experiments.

It can be shown that using the non-linear modelling presented in this paper, non-linear effects at piezo–beam systems subjected to weak electric field could be modelled in a qualitative correct manner. For a more exact quantitative determination of the non-linear parameters, further investigations will be necessary. In future work, experimental data will be more deeply explored and electrostriction will be included in the model.

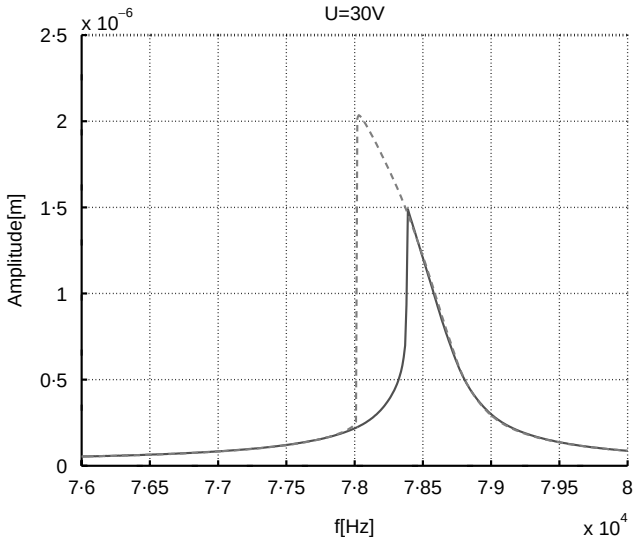

Figure 6. Longitudinal vibrations of PIC 181: jump phenomenon: —, sweep up experiment; — —, sweep down experiment.

REFERENCES

1. H. Cao and A. G. Evans 1993 *Journal of American Ceramic Society* **75**, 890–896. Nonlinear deformation of ferroelectric ceramics.
2. P. J. Chen and T. J. Tucker 1981 *Acta Mechanica* **38**, 209–218. Determination of the polar equilibrium properties of the ferroelectric ceramic PZT 65/35.
3. M. Kamlah 2001 *Continuum Mech. Thermodyn* **13**, 219–268. Ferroelectric and ferroelastic piezoceramics—Modeling of electromechanical hysteresis phenomena.
4. J. A. Main, E. Garcia and D. V. Newton *Journal of Guidance, Control and Dynamics* **8**, 1068–1073. Precision position control of piezoelectric actuators using charge feedback.
5. E. F. Crawley and J. de Luis 1987 *American Institute of Aeronautics and Astronautics Journal* **25**, 1373–1385. Use of piezoelectric actuators as elements of intelligent structures.
6. M. N. Nguyen 1999 *Dissertation, TU, Darmstadt*. Nichtlineares dynamisches Verhalten von Piezo-Balken-Systemem bei schwachem elektrischem Feld.
7. S. Atluri 1973 *Journal of Applied Mechanics* **40**, 121–126. Nonlinear vibrations of a hinged beam including nonlinear inertia effects.
8. D. A. Evensen 1968 *American Institute of Aeronautics and Astronautics Journal* **6**, 370–372. Nonlinear vibration of beams with various boundary conditions.
9. A. V. Srinivasan 1965 *American Institute of Aeronautics and Astronautics Journal* **10**, 1951–1953. Amplitude–free oscillations of beams and plates.
10. H. F. Tiersten 1969 *Linear Piezoelectric Plate Vibrations*. New York: Plenum Press.
11. U. von Wagner, P. Hagedorn and M. N. Nguyen 2001 *Proceedings of DETC 2001 ASME Conference, Pittsburgh*. Nonlinear behavior of piezo–beam-systems subjected to weak electric field.
12. A. H. Nayfeh and D. Mook 1979 *Nonlinear Oscillations*. New York: John Wiley and Sons Inc.
13. P. Hagedorn 1989 *Technische Schwingungslehre, Band II*. Springer, Berlin.
14. S. K. Parashar 2001 *Master Thesis, TU, Darmstadt*. Experimental investigation and finite element modelling of nonlinear vibration behavior of piezo–beam-systems.
15. M.-A. Weber, M. Kamlah and D. Munz *Experimente zum Zeitverhalten von Piezokeramiken* FZKA 6465. Report Forschungszentrum Karlsruhe.